DOI: 10.31401/WS.2023.proc.13



# Intense Mid-Latitude Magnetic Disturbances and Solar Wind Conditions

*Lubchich A.A.[1], Despirak I.V.[1], Werner R.[2]*

[1]Polar Geophysical Institute, Apatity, Russia, e-mail: lubchich@pgia.ru
[2]Space Research and Technology Institute, Bulgarian Academy of Sciences, Stara Zagora Department, Bulgaria

**Abstract**

The purpose of this work is to find out the solar wind conditions under which high values of magnetic disturbances at the middle latitudes are observed. The intensity of magnetic disturbances was determined according Midlatitude Positive Bay (MPB) index proposed by McPherron and Chu, 2017. The list of the MPB index dating back to 1991 and can be found in the supplementary information for the online version of McPherron and Chu, 2018. Calculations of MPB index is based on data from 41 stations in the northern and southern hemispheres (from 20° to 52° magnetic latitude). In additional, for several selected events, we analyzed the variations of horizontal component of magnetic field at the mid-latitudes stations (including the Panagjurishte station in Bulgaria). The study of the magnetic disturbances was based on the data from the magnetometer networks SuperMAG, INTERMAGNET and IMAGE. The solar wind conditions before the substorms were determined using the CDAWeb OMNI database (http://cdaweb.gsfc.nasa.gov/), the solar wind structures were determined according to the catalog of large-scale solar wind phenomena (ftp://ftp.iki.rssi.ru/omni/). It was found the dependences of occurrence of high values of MPB index on solar wind parameters (components of the interplanetary magnetic field, solar wind velocity, density, dynamic pressure etc.). Several examples of very intensive events are discussed.

**Keywords:** solar wind, magnetic substorm, Mid-latitude Positive Bay (MPB-index)

## Introduction

Our work is devoted to the study of intense mid-latitude magnetic bays appearance in dependence of solar wind and IMF conditions as well as on the magnetic storms and substorms development. It is known that the substorm development associated with substorm current wedge (SCW) formation [e.g., McPherron al., 1973; Sergeev et al., 2011]. The SWC produces a distinctive pattern of changes in the ground-based magnetic field components at the mid-latitudes: X- component of the magnetic field is positive and symmetric about the central meridian of the SCW, while the Y component is antisymmetric [Kepko et al., 2015]. The positive deviations in the Y- component occur if the substorm onset meridian is located far eastward, the negative Y values occur if the substorm onset is located westward [e.g., McPherron al., 1973; McPherron and Chu, 2018]. Recently, McPherron and Chu have introduced a new index - the Mid-latitude Positive Bay index (MPB), which characterized the intensity of SCW [McPherron and Chu, 2017].The list of the MPB index dating back to 1982 and can be found in the supplementary information for the online version of McPherron and Chu, 2018. In our work we use the list of the MPB index kindly provided by Chu [Chu et al., 2015]. Calculations of MPB index is based on data from 41 stations in the northern and southern hemispheres (from 20° to 52° magnetic latitude). Werner et al. (2021) proposed a modification of the calculation procedure, adding the data from the Bulgarian station Panagjurishte (PAG) (42.5°N, 24.2°E, ~37° GMLat; ~97º GMLon). Figure 1 shown the example of the daily MPB-index on 28 August 2018, the horizontal line marks the values of MPB-X= 10 000 nT$^2$ (i.e., intense variations in the X-component, $\Delta X$ = 100 nT).

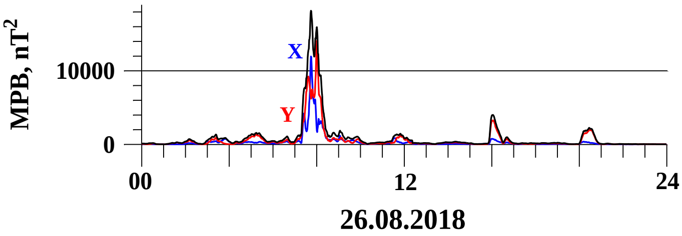


***Figure 1***. *MPB-index for August 28, 2018: MPB calculated only on X component (MPB-X) marked by blue line, only on Y- component (MPB-Y) – by red line, on X and Y components - by black line.*

## Data

The solar wind and IMF parameters are taken from OMNI database https://cdaweb.gsfc.nasa.gov/. Global magnetometer networks SuperMAG and IMAGE data were used for determination of the substorm development as at the midlatitudes well as at auroral latitudes. SML- index is taken from http://supermag.jhuapl.edu/. The IMAGE magnetometer data are taken from http://space.fmi.fi/image/. MPB index is taken from the Chu list [Chu et al., 2015]. It includes minute values of squared X and Y horizontal field variations and their sum, equal to total power in horizontal field variations, from 1991-01-01/00:00 to 2019-12-31/23:59.

## Results

### 1) The relationship between extreme values of the MPB index and magnetic storms

For this purpose, we selected all events in the period from 1991 to 2019, when MPB-X > 10 000 $nT^2$ (i.e., $\Delta X$ > 100 nT). MPB-X values were taken so that events developed at close longitudes. For comparison, the Table of superstorms was used (superstorm criterion: $Dst_{min}$ < -250 nT) [Meng et al., 2019]. We added the last column to this table, which indicates the maximum value of the MPB index, the date (month, day) and the time of the event.

| 1 | 2 | 3 | 4 | 5 | 6 | 7 | 8 |
|---|---|---|---|---|---|---|---|
| **Solar cycle** | $Dst_{min}$ time (yyyy-mm-dd UT) | $Dst_{min}$ (nT) | SYM-Hmin/time (nT)/(mm-dd UT) | SI+/time (nT)/(mm-dd UT) | Type | Interplanetary Case | MPB ($nT^2$)/(mm-dd UT) |
| SC23 | 2003-11-20 20:30 | -422 | -490/11-20 18:17 | 49/11-20 08:06 | III | Sheath+MC Bxz- | ~69 000/11-20 17:03 |
| SC23 | 2001-03-31 08:30 | -387 | -437/03-31 08:06 | 129/03-31 01:00 | I | Sheath+MC Bxzc- | ~26 000/03:31 06:09<br>~21 000/03:31 15:53 |
| SC23 | 2003-10-30 22:30 | -383 | -432/10-30 22:55 | 76/10-30 20:08 | III | Sheath | ~46 000/10-30 21:35 |
| SC23 | 2004-11-08 06:30 | -374 | -394/11-08 05:55 | 92/11-07 19:20 | I | Sheath+MC Bxz- | ~27 000/11-08 01:19<br>[MPB X~9 300] |
| SC22 | 1991-11-09 01:30 | -354 | -402/11-09 01:32 | 49/11-08 13:15 | I | Unknown | ~575000/11-08 22:20 |
| SC23 | 2003-10-30 00:30 | -353 | -391/10-30 01:48 | 81/10-29 06:14 | III | Sheath+MC Bxz- | ~69000/10-29 19:56 |
| SC23 | 2000-07-16 00:30 | -301 | -347/07-15 21:54 | 93/07-15 15:04 | II | MC Bxz- | ~23000/07-15 21:48 |
| SC22 | 1991-03-25 00:30 | -298 | -337/03-25 03:41 | 118/03-24 03:55 | II | Unknown | ~105000/03-24 21:33<br>~24000/03-24 04:06 |
| SC23 | 2001-11-06 00:30 | -292 | -320/11-06 04:06 | 88/11-06 01:54 | II | PICME+sheath | ~11000/11-06 02:05<br>[MPB X~6 300] |
| SC22 | 1992-05-10 14:30 | -288 | -363/05-10 14:15 | 81/05-09 20:02 | II | Likely sheath+MC | ~28000/05-10 18:29 |
| SC23 | 2000-04-07 00:30 | -288 | -320/04-07 00:09 | 46/04-06 16:45 | III | Sheath | ~60000/04-06 23:27 |
| SC23 | 2001-04-11 23:30 | -271 | -280/04-11 23:57 | 26/04-11 15:53 | III | Sheath | ~24000/04-11 21:37<br>~23000/04-12 00:16 |
| SC23 | 2004-11-10 10:30 | -263 | -282/11-10 09:31 | 46/11-09 18:51 | III | Sheath+MC Bxz+ | ~31000/11-09 20:32 |
| SC22 | 1991-10-29 07:30 | -254 | -284/10-29 08:02 | 51/10-28 11:03 | III | Sheath+MC Bxz+ | ~223000/10-28 16:06 |

***Table 1***. *Table of superstorms (was taken from Meng et al.,2019) and added MPB >10 000 $nT^2$.*

It is seen that most of extreme MPB events took place during superstorms. In addition, it turned out that the remaining events of extreme MPB were also observed during magnetic storms (Dst < -100 nT). This result shown in the Table 2, the format of Table 2 is the same of Table 1. The first storm ($Dst_{min}$ = -247 nT) is disputable, someone also relates it to superstorms.

| **Solar cycle** | **$Dst_{min}$ time (yyyy-mm-dd UT)** | **$Dst_{min}$ (nT)** | **SYM-Hmin/time (nT)/(mm-dd UT)** | **SI+/time (nT)/(mm-dd UT)** | **Type** | **Interplanetary Case** | MPB ($nT^2$)/(mm-dd UT) |
|---|---|---|---|---|---|---|---|
| SC23 | *2005-05-15 08:30 | -247 | -305/05-15 08:20 | 62/05-15 02:41 | I | Sheath+MC | ~38 000/05-15 08:50 |
| SC22 | 1991-06-05 19:30 | -223 | -238/06-05 16:56 | 30/06-04 15:39 | II | | ~50 000/06-05 17:14 |
| SC23 | 2001-11-24 16:30 | -221 | -234/11-24 12:37 | 86/11-24 06:04 | III | Sheath(M)+ICME | ~49 000/10-30 07:15 |
| SC22 | 1991-11-01 23:30 | -196 | -200/11-01 19:37 20:22 | 21/11-01 12:00 | II | | ~36 000/11-01 20:30 |
| SC22 | 1991-07-13 15:30 | -183 | -238/07-13 15:42 | 47/07-13 08:26 | I | | ~42 000/07-13 16:20 |
| SC23 | 2002-10-01 16:30 | -176 | -154/10-01 12:53 | 26/09-30 8:26 (?) | III | Sheath+MC+CIR | ~18 000/10-01 16:28 |
| SC24 | 2018-08-26 06:30 | -175 | -206/08-26 07:11 | 11/08-25 12:31 (?) | I | MC+CIR | ~18 000/08-26 07:44 |
| SC22 | 1992-02-26 22:00 | -174 | -167/02-26 22:31 | 35/02-26 17:02 | I | | ~61 000/02-26 19:44 |
| SC22 | 1992-02-08 16:30 | -114 | -126/02-08 15:18 | 33/02-08 14:32 | I | | ~41 000/02-08 15:35 |

***Table 2***. *Table of magnetic storms with Dst < -100 nT and extreme MPB events.*

### 2) MPB index distribution and their correlations with geomagnetic indexes

To conduct a statistical analysis of the MPB index, we took the entire data series for the MPB from 1991 to 2019, regardless of its value. During the same time, one-minute values of geomagnetic indices for different latitudes were taken: low-latitudes index SYM-H, mid-latitudes index ASY-H; auroral index AL, universal index SML and high-latitudes index PC(N). We carried out a statistical analysis of these data series and obtained the distributions of the MPB, SML, AL, SYM-H, ASY-H, and their possible correlations, some results are presented in Figure 2.

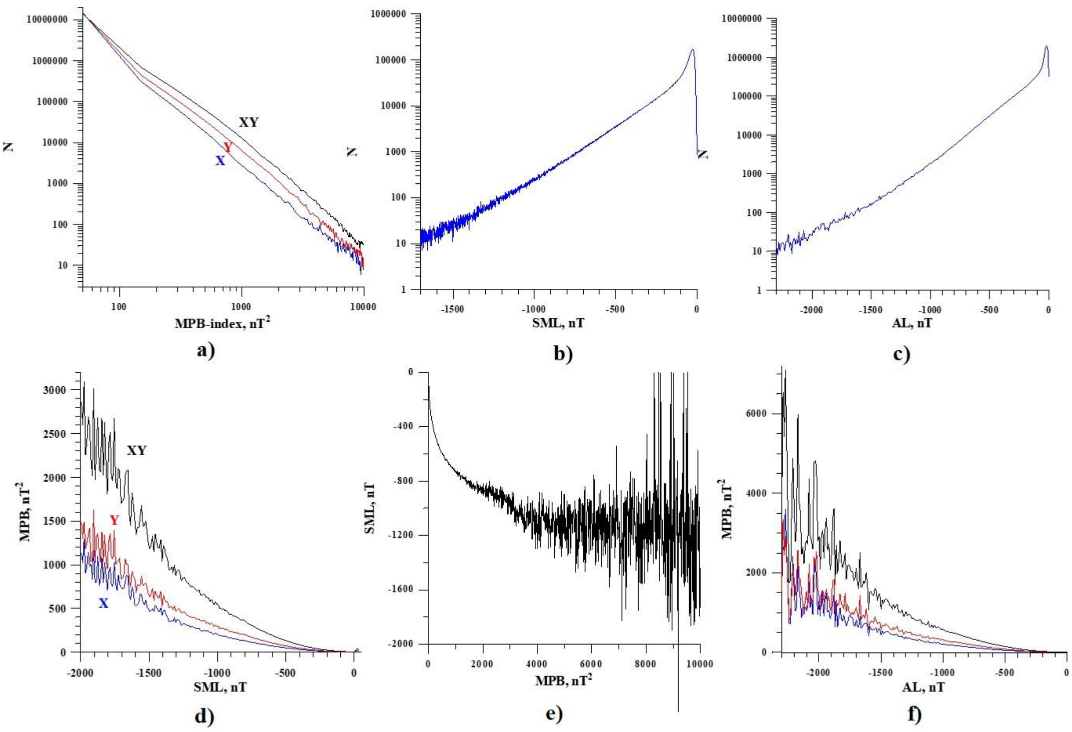


***Figure 2.*** *Distributions of the MPB (a), SML (b), AL (c); dependence of MPB on SML (d) and vice versa (e), on AL (f).*

It is seen that the distributions of geomagnetic indices, as well as most SW and IMF parameters (Figure 3 and 4) are far from normal (Gaussian) distributions. Therefore, if for two quantities A and B we construct the dependences A(B) and B(A), then they, in the general case, will not coincide and may even differ greatly. For example, this can be seen in Figure 2d and 2e, the dependences of the MPB(SML) and SML(MPB). Recently, Werner et al. (2023), having analyzed the distributions of the geomagnetic IL index for the interval 2007–2020, also found that this distribution is not Gaussian, but is well described by exponential functions, in particular, by the Weibull distribution.

From Figure 2 it is seen that the more disturbed the geomagnetic conditions, the higher the MPB index. So, the MPB index strongly depends on the value of SML. As SML decreases from 0 to -2000 nT, the MPB increases from 0 to about 2500 $nT^2$. There is observed also an inverse relationship: with an increase of MPB-index from 0 to 3000 $nT^2$, the SML-index decreases from the maximum value to approximately -900 nT, with a further increase in MPB, SML decreases slightly (but in this region there are few events).

It should be noted that the dependence of the MPB on all geomagnetic indices, which is similar in form, can be explained as follows: in the analyzed time interval, all indices are approximately related by a linear dependence:

AL ≈ 0.81 * SML -26.5;
ASY-H ≈ -0.086 * SML + 3.14;
SYM-H ≈ 0.073 * SML + 1.31;
PC(N) ≈ -0.0051 * SML + 0.66.

### 3) MPB index correlations with the solar wind and IMF parameters

To conduct the analysis of the correlations between the MPB index and different solar wind parameters, the entire data series for the MPB-index and one-minute values of solar wind and IMF parameters were taken: the magnitude of the IMF and its components, solar wind velocity and its components, density, temperature, dynamic pressure etc.

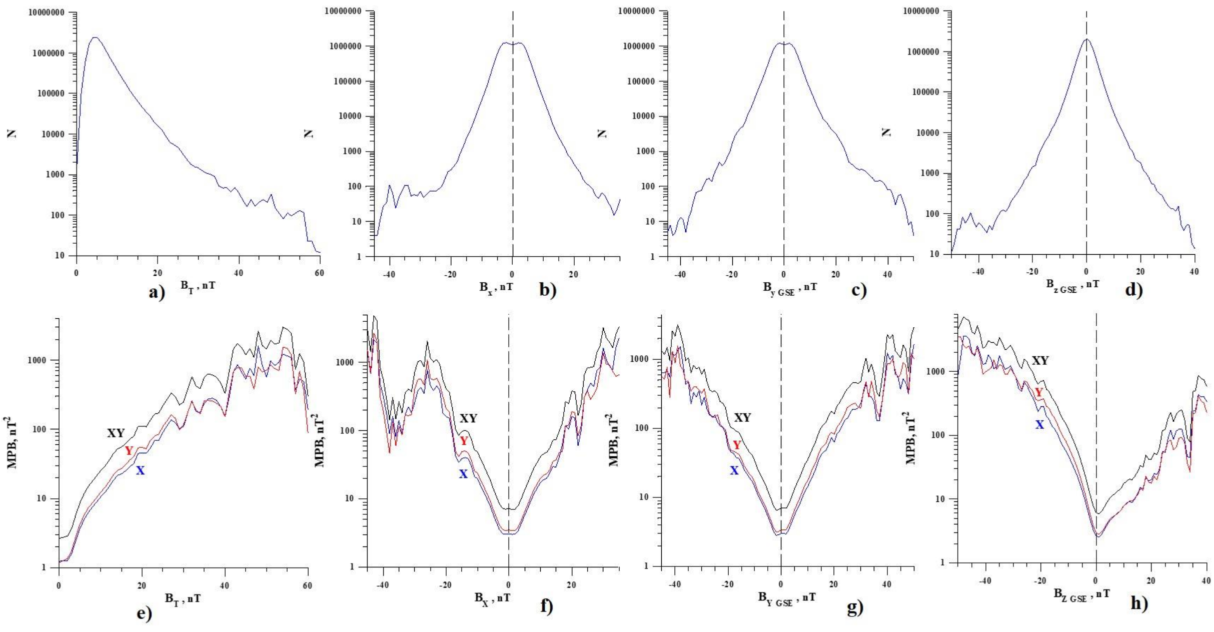


***Figure 3****. Distributions of the magnitude of the IMF and its components- $B_T$ (a), $B_X$ (b), $B_Y$ (c), $B_Z$ (d); dependence of MPB on $B_T$ (e), $B_X$ (f), $B_Y$ (g) and $B_Z$ (h).*

We carried out a statistical analysis of these data series and obtained the distributions of the parameters of the solar wind and IMF and all possible correlations, some results are presented in Figures 3 and 4.

At the top panels of Figure 3 (a, b, c, d) shown the distributions of modulus of the IMF ($B_T$) and all IMF components ($B_X$, $B_Y$, $B_Z$). It is seen that the distributions of all IMF components are more or less symmetrical with respect to zero values. The distribution of the IMF modulus ($B_T$) reaches a maximum at 4–5 nT, then gradually decreases. At the bottom panels of Figure 3 (e, f, g, h) shown the dependences of the MPB index on the interplanetary magnetic field (IMF). The MPB index grows with the growth of the IMF modulus. The MPB index also grows with an increase in the modulus of the IMF components. For the $B_X$ and $B_Y$ components of the IMF, the dependence is more or less symmetrical. For the $B_Z$-component, as expected, the dependence is asymmetric, because the MPB index is more dependent on the negative values of the $B_Z$.

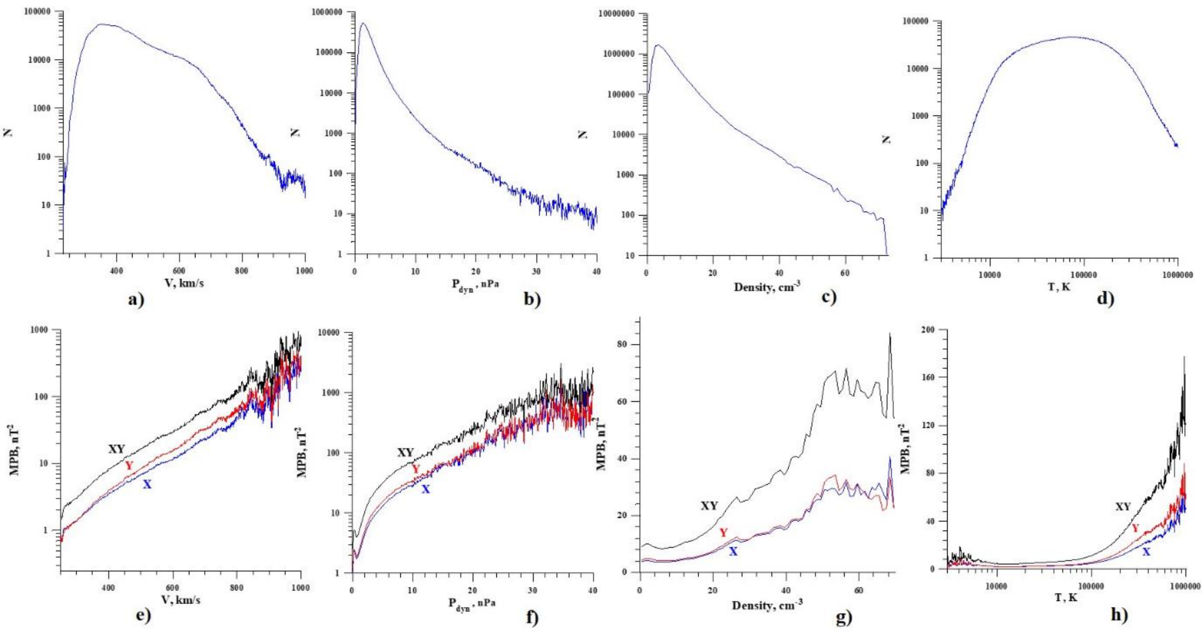


***Figure 4***. *Distributions of the V (a), $P_{dyn}$ (b), density (c), T (d); dependence of MPB on V (e), $P_{dyn}$(f), density (g) and T (h)*

On the Figure 4 shown the distributions of solar wind parameters and their dependences of the MPB index, the format of Figure 4 is the same as Figure 3. It is seen that the distribution of the solar wind velocity increases sharply with increasing V, reaches the maximum at ~ 350 km/s, then gradually decreases. The distribution of temperature (in the picture was presented ln(T)) is more or less symmetrical with respect to value T = 70000 K. The distributions of the density and the dynamic pressure initially increase sharply, reach maximums at N~ 3.5 cm$^{-3}$ and $P_{dyn}$ ~1.3 nPa, and then gradually decrease.

At the bottom panels of Figure 4 (e, f, g, h) shown the dependences of the MPB index on the solar wind velocity V, dynamic pressure $P_{dyn}$, density N and temperature T. It is seen that the MPB index grows almost exponentially with the grow of the solar wind velocity V. That is, the dependence of the ln(MPB) on module of the velocity V is close to linear. An almost similar dependence on the solar wind dynamic pressure (the dependence of the ln(MPB) on the $P_{dyn}$) is close to linear by $P_{dyn}$ > 6 nPa. The MPB index also strongly depends on the electric field of the solar wind (not shown at the Figure 4).

Although the MPB increases with an increase of the solar wind density and solar wind temperature T, these dependences are very weak (i.e. when these values change, the MPB index changes in a small interval).

**Summary**

The one-minute values of the Midlatitude Positive Bay index for 19 years, from 1991 to 2019, were analyzed. It was found that:

- All extremely high values of the MPB index (MPB > 10 000 $nT^2$) were observed during magnetic storms with $Dst_{min}$ < -100 nT.
- All superstorms ($Dst_{min}$ < -250 nT) were accompanied by extremely high values of the MPB index.
- The MPB index increases with increasing in the level of geomagnetic activity. The higher the -SML, -SYM-H, -ASY-H, -AL, AE index or the absolute value of PC(N)-index, the on average higher the MPB index.
- The MPB index increases with increasing the IMF magnitude and the absolute values of interplanetary magnetic field components.
- The MPB index rapidly increases with increasing the solar wind speed and dynamic pressure. The MPB index is less dependent on the density and temperature of the solar wind.

**Acknowledgments**

This study was supported by the RFBR (project number 20-55-18003) and National Science Fund of Bulgaria (NSFB) (project number КП-06-Русия/15).

**References**

Chu, X., McPherron, R.L., Hsu, T.S., Angelopoulos, V. (2015). Solar cycle dependence of substorm occurrence and duration: Implications for onset, J. Geophys. Res.: Space Physics, Vol. 120, pp. 2808 - 2818, DOI: 10.1002/2015JA021104.

Kepko, L, McPherron, R.L., Amm, O., Apatenkov, S., Baumjohann, W., Birn, J., Lester, M., Nakamura, R., Pulkkinen, T.I., Sergeev, V.A. (2015). Substorm Current Wedge Revisited, Space Sci. Rev., Vol. 190, pp. 1–46, https://doi.org/10.1007/s11214-014-0124-9

McPherron, R.L., Chu, X. (2018). The midlatitude positive bay index and the statistics of substorm occurrence, J. Geophys. Res.: Space Physics, Vol. 123, No. 4, pp. 2831–2850, https://doi.org/10.1002/2017JA024766

McPherron, R.L., Chu, X., (2017). The midlatitude positive bay and the MPB index of substorm activity, Space Sci. Rev., Vol. 206(1–4), pp. 91–122.

McPherron, R.L., Russell, C.T., Aubry, M.P. (1973). Satellite studies of magnetospheric substorms on August 15, 1968: 9. Phenomenological model for substorms, J. Geophys. Res., Vol. 78, No. 16, pp. 3131-3149, https://doi.org/10.1029/JA078i016p03131

Meng, X., Tsurutani, B.T., Mannucci, A.J. (2019). The Solar and Interplanetary Causes of Superstorms (Minimum Dst ≤ −250 nT) During the Space Age. J. Geophys. Res.: Space Physics, Vol. 124, No. 6, pp. 3926-3948, https://doi.org/10.1029/2018JA026425

Sergeev, V.A., Angelopoulos, V., Kubyshkina, M., Donovan, E., Zhou, X.-Z., Runov, A., Singer, H., McFadden, J., Nakamura, R. (2011). Substorm growth and expansion onset as observed with ideal ground-spacecraft THEMIS coverage, J. Geophys. Res., Vol. 116, A00I2, https://doi.org/10.1029/2010JA015689

Werner, R., Guineva, V., Atanassov, A., Bojilova, R., Raykova, L., Valev, D., Lubchich, A., Despirak, I. (2021). Calculation of the horizontal power perturbations of the Earth surface magnetic field, Proceedings of the Thirteenth Workshop "Solar Influences on the Magnetosphere, Ionosphere and Atmosphere", September, 2021, Book of Proceedings, pp. 159-165, DOI: 10.31401/WS.2021.proc.

Werner, R., Guineva, V., Despirak, I.V., Lubchich, A.A., Setsko, P.V., Atanassov, A., Bojilova, R., Raykova, L. Valev, D. (2023). Statistical Studies of Auroral Activity and Perturbations of the Geomagnetic Field at MiddleLatitudes, Geomagnetism and Aeronomy, Vol. 63, No. 4, pp. 473–485, DOI: 10.1134/S0016793223600303.